

Temperature Dependence of Switching of the Bacterial Flagellar Motor by the Protein CheY^{13DK106YW}

Linda Turner,*† Aravinthan D. T. Samuel,*† Alan S. Stern,† and Howard C. Berg*†

*Department of Molecular and Cellular Biology, Harvard University, Cambridge, Massachusetts 02138, and the †Rowland Institute for Science, Cambridge, Massachusetts 02142 USA

ABSTRACT The behavior of the bacterium *Escherichia coli* is controlled by switching of the flagellar rotary motor between the two rotational states, clockwise (CW) and counterclockwise (CCW). The molecular mechanism for switching remains unknown, but binding of the response regulator CheY-P to the motor component FliM enhances CW rotation. This effect is mimicked by the unphosphorylated double mutant CheY^{13DK106YW} (CheY^{**}). To learn more about switching, we measured the fraction of time that a motor spends in the CW state (the CW bias) at different concentrations of CheY^{**} and at different temperatures. From the CW bias, we computed the standard free energy change of switching. In the absence of CheY, this free energy change is a linear function of temperature (Turner et al., 1996. *Biophys. J.* 71:2227-2233). In the presence of CheY^{**}, it is nonlinear. However, the data can be fit by models in which binding of each molecule of CheY^{**} shifts the difference in free energy between CW and CCW states by a fixed amount. The shift increases linearly from $\sim 0.3kT$ per molecule at 5°C to $\sim 0.9kT$ at 25°C, where k is Boltzmann's constant and T is 289 Kelvin (= 16°C). The entropy and enthalpy contributions to this shift are about $-0.031kT/^\circ\text{C}$ and $0.10kT$, respectively.

INTRODUCTION

The chemotactic behavior of the motile bacterium *Escherichia coli* depends on the direction of rotation of its flagellar motors. Each motor behaves as a two-state system, spinning alternately clockwise (CW) and counterclockwise (CCW). For general reviews of bacterial motility and chemotaxis, see Blair (1995), Macnab (1996), Stock and Surette (1996), and Falke et al. (1997). For reviews on the flagellar switch, see Macnab (1995), Eisenbach and Caplan (1998), and Silversmith and Bourret (1999).

At fixed concentrations of chemical attractants, the probabilities per unit time (rates) of transitions between CW and CCW states are constant, and CW and CCW interval distributions are exponential (Block et al., 1983). Addition of attractant reduces the level of phosphorylation of a response regulator CheY-P, shortening CW intervals and lengthening CCW intervals (Hess et al., 1987, 1988; Oosawa et al., 1988; Wylie et al., 1988). CheY-P binds to a component at the base of the motor, FliM (Welch et al., 1993, 1994). This binding stabilizes the CW state and destabilizes the CCW state. This has been shown both for the native protein CheY-P (Alon et al., 1998) and for the double mutant CheY^{13DK106YW} (CheY^{**}) (Scharf et al., 1998). The latter protein can be phosphorylated to some extent but is active without phosphorylation.

In cells in which the cytoplasm has been exchanged for buffer (Ravid and Eisenbach, 1984), or in which CheY (Liu

and Parkinson, 1989) or CheY and other cytoplasmic chemotaxis proteins have been deleted (Wolfe et al., 1987; Abouhamad et al., 1998), motors spin exclusively CCW. In the former case, switching between CW and CCW states can be induced by the addition of fumarate, which stabilizes the CW state (Prasad et al., 1998). In the latter case, switching can be induced simply by lowering the temperature (Turner et al., 1996). In the work reported here, we have repeated these temperature-dependence experiments in cells that express the double mutant CheY^{**}.

The results are interpreted using models in which the binding of each molecule of CheY^{**} shifts the difference in free energy between CW and CCW states by a fixed amount. In one, the Monod-Wyman-Changeux (MWC) model, the motor's behavior is analyzed in terms of differential binding, the dissociation constant for the CW state being about a factor of 2 smaller than the constant for the CCW state (Monod et al., 1965; Alon et al., 1998). In the other, the Scharf model, binding is characterized by a single dissociation constant, and the relative free energy change between the two states is used as an additional parameter (Scharf et al., 1998). The two models yield similar results.

MATERIALS AND METHODS

Chemicals

Chemicals were obtained from the following sources: Apiezon grease M, Apiezon Products (London, England); bacto-tryptone, yeast extract, Difco Laboratories (Detroit, MI); glycerol, sodium chloride (enzyme grade), Fisher Scientific (Pittsburgh, PA); isopropyl β -D-thiogalactoside (IPTG), Gold Biotechnology (St. Louis, MO); potassium phosphate dibasic trihydrate, potassium phosphate monobasic anhydrous, dipotassium salt of EDTA, sodium salt of ampicillin, Sigma Chemical Co. (St. Louis, MO); Rain-X, Unelco Corporation (Scottsdale, AZ). Water was deionized (18 M Ω -cm) and filtered (0.2 μm).

Received for publication 23 December 1998 and in final form 26 April 1999.

Address reprint requests to Dr. Howard C. Berg, Molecular and Cellular Biology, Harvard University, 16 Divinity Ave., Cambridge, MA 02138. Tel.: 617-495-0924; Fax: 617-496-1114; E-mail: hberg@biosun.harvard.edu.

© 1999 by the Biophysical Society

0006-3495/99/07/597/07 \$2.00

Equipment

A phase-contrast microscope (Nikon Optiphot-2) was equipped with a CCD camera (Marshall Electronics model V1070) run with a shutter setting of 1 ms. The video signal was sent to a video cassette recorder (Panasonic model AG6730 with Sony PVM-96 monitor) via a homemade time generator, for analysis frame by frame by eye, and to a PC equipped with a Hobson Rotation Tracking System (Oxford, England), for analysis by computer.

Temperature control

The microscope objective and the stage were controlled with the same Peltier element, as described previously (Khan and Berg, 1983). The temperature of the flow cell was monitored with a thermistor calibrated with a mercury thermometer certified by the National Institute of Standards and Technology. The microscope objective, stage, and temperature-control element were housed in a plexiglass box containing a dessicant, to reduce convection and eliminate condensation.

Bacterial cultures

Strain HCB902 carries in single copy *cheY*^{Y13DK106YW} under control of the promoter Ptrc (inducible by IPTG) as a replacement for wild-type *cheY*, on a chromosome deleted for *cheA* and *cheZ* (Scharf et al., 1998). It was grown overnight from -75°C frozen glycerol stocks in a 125-ml culture flask containing 10 ml TB (1% Bacto-tryptone, 0.5% NaCl), 0.1% yeast extract, and 100 $\mu\text{g/ml}$ ampicillin. Bacteria for a day's experiment were grown by diluting the saturated culture 1:200 in a 125-ml flask containing TB and 100 $\mu\text{g/ml}$ ampicillin. After 4 h, IPTG from a freshly thawed 0.01 M stock solution was added (final concentration 0, 15, or 30 μM), and incubation was continued for 2 h, after which the OD₆₁₀ of the culture was ~ 0.8 . All incubations were at 33°C with rotary shaking at 200 rpm.

Tethering

For behavioral assays we used a flow cell (Berg and Block, 1984) equipped with a glass tethering surface silanized with a commercial product, Rain-X, and held in place with Apiezon grease M. The bacteria were sheared (Berg and Turner, 1993) 45 times and added to the flow cell. The flow cell was inverted for 10 min and then rinsed with many volumes of buffer solution: 10 mM potassium phosphate (pH 7), 67 mM sodium chloride, 0.1 mM EDTA.

Data acquisition

Cells were grown at different concentrations of IPTG, tethered, and examined in the microscope. Beginning at the ambient temperature (22°C), close to the temperature of the experiments of Scharf et al. (1998), CW biases and reversal rates were measured. The temperature was then ramped up or down in steps with repeated measurements. The first measurement at 22°C was repeated at the end of a series of temperature changes and frequently again during an extended set of measurements. The CW bias for each cell returned to a value close to its initial value. Data were collected for a period up to 4 h, for intervals of 4–6 min at each temperature for each cell. Bias and reversal frequency determined by eye and by the Hobson Rotation Tracker agreed, provided that the smoothing functions for the Hobson Rotation Tracker were set appropriately.

Data analysis

The output of the Hobson Rotation Tracker is a list of sequential time intervals of CW, CCW, and indeterminate rotation. The first and last

intervals and the intervals of indeterminate rotation, which were infrequent, were deleted. We calculated the CW bias as the (time span of all CW intervals)/(total time span), the reversal frequency as the (total number of intervals)/(total time span), and the rates k_+ as (reversal frequency)/[2(1 – CW bias)], and k_- as (reversal frequency)/[2(CW bias)]. The mean bias at 22°C was used to determine the CheY** concentration of a cell, according to the solid line of figure 3 A in Scharf et al. (1998).

RESULTS

As explained in Materials and Methods, the mean bias at 22°C was used as a measure of the concentration of CheY** for each cell. We assumed that this concentration did not change with temperature and that variations in CW bias from cell to cell were due to differences in the concentration of CheY**, not to differences in responsiveness of individual flagellar motors. The biases and reversal frequencies are shown in the left and middle columns of Fig. 1. At 22°C , each dot corresponds to the average of the bias measurements for a cell; at other temperatures, each dot corresponds to a single bias measurement. To simplify the analysis, the cells were grouped according to bias at 22°C (and by inference, CheY** concentration). The group averages for bias and reversal frequency are shown by the open symbols in the left and middle columns of Fig. 1, and the transition rate constants computed from them by the open and closed symbols in the right column of Fig. 1. The solid and dashed lines are fits to the models and are discussed below.

The CW biases for the different groups of cells are shown as a function of temperature in Fig. 2 A, for all temperatures assayed. Closed circles indicate the data obtained earlier for cells without CheY (Turner et al., 1996). If the CW bias was low at room temperature (<0.4), it increased as the temperature was lowered. If the CW bias was high at room temperature (>0.7), it decreased slowly as the temperature was lowered and decreased quite rapidly as the temperature was raised. The corresponding differences in standard free energy between CCW and CW states, calculated as $\Delta G^{\circ} = kT \ln[(1 - \text{CW bias})/(\text{CW bias})]$, are shown in Fig. 2 B. In the absence of CheY, the standard free energy change for switching increases linearly with temperature. In the presence of CheY**, matters are more complex.

One of our goals was to quantify the enthalpic and entropic contributions to the free energy change of switching for different amounts of CheY**. The nonlinearity of the data prohibited a van't Hoff analysis of the standard free energy change into components $\Delta G^{\circ} = \Delta H^{\circ} - T\Delta S^{\circ}$. Although it is possible to fit the data using a regression analysis based on a quadratic expression of the temperature dependence of the free energy change (Osborne et al., 1976; Waelbroeck et al., 1979), the implications of such a fit are not clear. Instead, we used the models described in the next section to estimate both the dissociation constants and the standard free energy shift of switching due to binding of each CheY** to the motor.

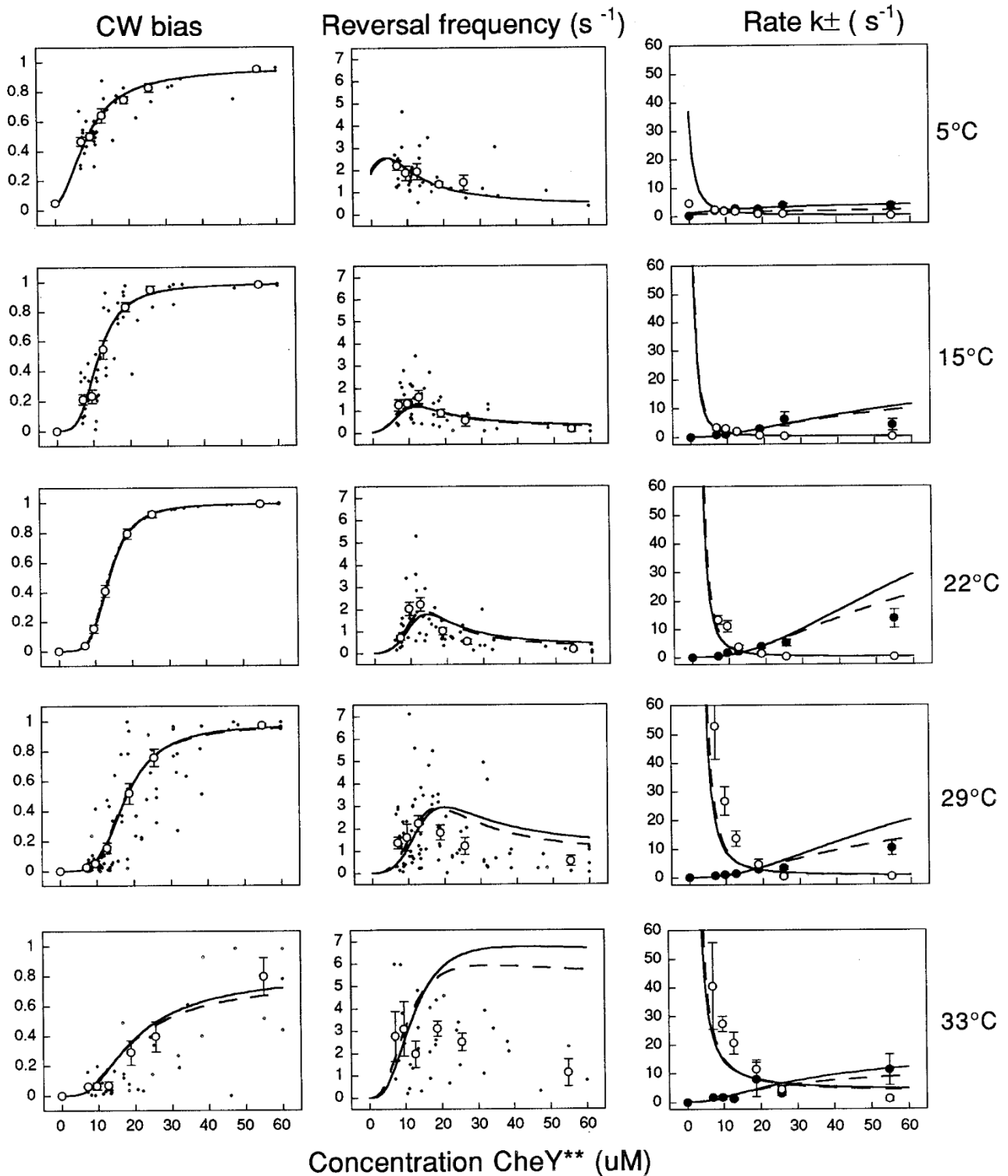


FIGURE 1 Measurements of CW bias (*left column*), reversal frequency (*middle column*), and transition rate constants (*right column*) shown at five different temperatures. At 22°C, each \cdot corresponds to the mean bias at that temperature, with the CheY** concentration estimated according to Scharf et al. (1998), as explained in the text. At other temperatures, each \cdot corresponds to a bias measurement. Cells of similar bias (at 22°C) were grouped, and a common CheY** concentration was estimated from the mean bias for that group. The open symbols shown in the left and middle columns are plotted at the concentrations thus determined, at heights corresponding to the bias or reversal rate for that group, with the error bar representing the standard error. The rate constants k_+ (CCW to CW, \bullet) and k_- (CW to CCW, \circ) shown in the right column were computed from the group values for CW bias and the reversal rate shown in the left and middle columns, respectively; see Materials and Methods. The CW bias for each group at 22°C (mean \pm standard error), the corresponding estimate for CheY** concentration (μM), and the number of measurements in each group were 0.04 ± 0.01 , 12.7, 27; 0.15 ± 0.03 , 9.6, 28; 0.41 ± 0.04 , 12.7, 21; 0.79 ± 0.04 , 18.8, 28; 0.92 ± 0.02 , 25.6, 28; and 0.99 ± 0.01 , 54.9, 9. The number of cells studied is 64. The solid and dashed lines are fits to the models of Monod et al. (1965) and Scharf et al. (1998), respectively.

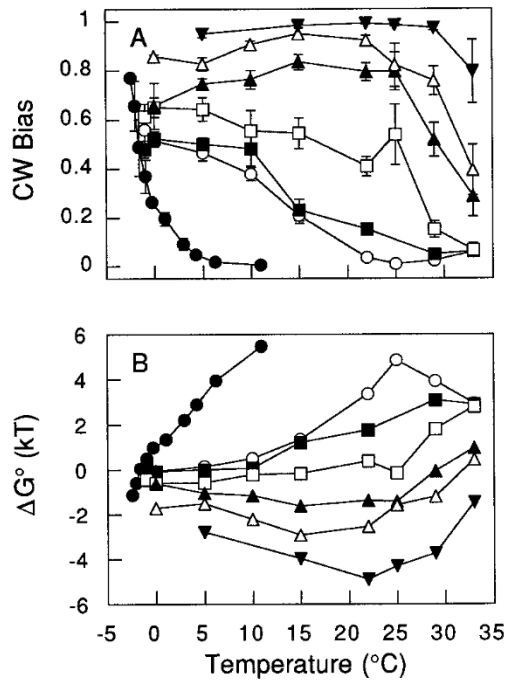
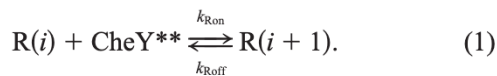


FIGURE 2 CW bias (A) and the standard free energy change for switching (B) shown as a function of temperature. The CheY** concentrations (in μM) for the different cell groups (Fig. 1) were (●) 0 (data from Turner et al., 1996), (○) 7.1, (■) 9.6, (□) 12.7, (▲) 18.8, (△) 25.6, and (▼) 54.9.

MODELS

We will begin by rederiving some classical relationships of macromolecular binding (Tanford, 1961), adopting the terminology and notation used by Monod et al. (1965) in their model for concerted allosteric transitions. (Our treatment differs from theirs in that we explicitly allow the motor to change state regardless of how many molecules of CheY** are bound, as in the model proposed by Alon et al. (1998).) The two states of the motor are called the R state (CCW) and the T state (CW)—as a convenient mnemonic, note that the R state corresponds to a run and the T state to a tumble. $R(i)$ will refer to the motor in the R state with i CheY** molecules bound, and similarly for $T(i)$. Binding at each site is described by the reaction



(Here and below, we only write formulas for the R state, but the analogous T state formulas hold as well.) Under the assumption that binding is noncooperative, the values of the rate constants k_{Ron} and k_{Roff} are independent of i and of which sites are occupied. Let m be the total number of binding sites in the motor. The appropriate equilibrium equation is then

$$(m-i)k_{\text{Ron}}[R(i)][\text{CheY}^{**}] = (i+1)k_{\text{Roff}}[R(i+1)]. \quad (2)$$

It follows that the dissociation constants K_{R} and K_{T} are given by

$$K_{\text{R}} = \frac{k_{\text{Roff}}}{k_{\text{Ron}}} = \frac{m-i}{i+1} \frac{[R(i)][\text{CheY}^{**}]}{[R(i+1)]}. \quad (3)$$

Define $p_{\text{R}}(i)$ and $p_{\text{T}}(i)$ as the probabilities that a motor is in the R or T state with i CheY** molecules bound, i.e.,

$$p_{\text{R}}(i) = \frac{[R(i)]}{[R] + [T]}, \quad (4)$$

where $[R] = \sum_i [R(i)]$, and similarly for $[T]$. With $C = [\text{CheY}^{**}]$, Eq. 3 can be rewritten as

$$p_{\text{R}}(i+1) = \frac{m-i}{i+1} \frac{C}{K_{\text{R}}} p_{\text{R}}(i). \quad (5)$$

By induction,

$$p_{\text{R}}(i) = \binom{m}{i} \left(\frac{C}{K_{\text{R}}}\right)^i p_{\text{R}}(0). \quad (6)$$

Hence the probability that a motor is in the R state is

$$p_{\text{R}} = \sum_{i=0}^m p_{\text{R}}(i) = (1 + C/K_{\text{R}})^m p_{\text{R}}(0), \quad (7)$$

so the equilibrium constant for the R-T transition is

$$K_{\text{EQ}} = \frac{[T]}{[R]} = \frac{p_{\text{T}}}{p_{\text{R}}} = \left(\frac{1 + C/K_{\text{T}}}{1 + C/K_{\text{R}}}\right)^m L, \quad (8)$$

where the “allosteric constant” (Monod et al., 1965) L is $p_{\text{T}}(0)/p_{\text{R}}(0)$, i.e., L is the equilibrium constant in the absence of CheY**.

The log of the equilibrium constant is

$$\ln(K_{\text{EQ}}) = \ln L + m \ln \frac{1 + C/K_{\text{T}}}{1 + C/K_{\text{R}}}. \quad (9)$$

The analogous equation derived by Scharf et al. (1998) is

$$\ln(K_{\text{EQ}}) = \ln L + m \frac{r}{k_{\text{T}} C + K}, \quad (10)$$

where r is the negative of the change in the standard free energy of switching that occurs upon binding one molecule of CheY**, equivalent to $kT \ln(K_{\text{R}}/K_{\text{T}})$, and K is the dissociation constant for CheY**, equivalent to a weighted average of K_{R} and K_{T} . L was measured at a series of temperatures by Turner et al. (1996); the values obtained there have been extrapolated to the temperatures used in this study (assuming constant values for ΔH and ΔS). The value of m was taken to be 26 (Jones et al., 1990; Sosinsky et al., 1992).

With two further assumptions, it is possible to model the rates of the R-T transition. Let $k_{+}(i)$ and $k_{-}(i)$ be the rates at which a motor with i CheY** molecules bound switches respectively to or from the T state. The principle of detailed

balance requires that

$$k_+(i)p_R(i) = k_-(i)p_T(i). \quad (11)$$

Substituting this into Eq. 6 yields

$$k_+(i) \binom{m}{i} \left(\frac{C}{K_R}\right)^i p_R(0) = k_-(i) \binom{m}{i} \left(\frac{C}{K_T}\right)^i p_T(0). \quad (12)$$

The first assumption is that $\mu = k_+(i+1)/k_+(i)$ and $\nu = k_-(i+1)/k_-(i)$ are constants independent of i . Dividing Eq. 12 into the corresponding equation for $i+1$, we obtain

$$\mu/K_R = \nu/K_T, \quad (13)$$

which means that μ and ν are not independent values. (Note: it is possible to identify $-kT \ln(\mu)$ as the change in the activation energy of switching per molecule of CheY**.)

The second assumption is that the rates of CheY** binding and unbinding are much faster than the rates of switching. This is clearly true if binding is diffusion limited (see Scharf et al., 1998). Furthermore, if it were not true, then the distributions of CW and CCW intervals would not be exponential, but multiexponential. It follows that the rates k_+ and k_- of switching are simply averages over the $k_+(i)$ and $k_-(i)$ rates, weighted by the probabilities $p_R(i)$ and $p_T(i)$, respectively. Hence

$$k_+ = \frac{\sum_{i=0}^m k_+(i)p_R(i)}{\sum_{i=0}^m p_R(i)}, \quad (14)$$

and likewise for k_- . Using Eq. 6 and the fact that $k_+(i) = \mu^i k_+(0)$, this becomes

$$k_+ = \frac{\sum_{i=0}^m k_+(0)\mu^i \binom{m}{i} \left(\frac{C}{K_R}\right)^i p_R(0)}{\sum_{i=0}^m \binom{m}{i} \left(\frac{C}{K_R}\right)^i p_R(0)} = k_+(0) \left(\frac{1 + \mu C/K_R}{1 + C/K_R}\right)^m. \quad (15)$$

The analogous equation for k_- is

$$k_- = k_-(0) \left(\frac{1 + \nu C/K_T}{1 + C/K_T}\right)^m = k_-(0) \left(\frac{1 + \mu C/K_R}{1 + C/K_T}\right)^m, \quad (16)$$

where the last step uses Eq. 13. Consequently,

$$\ln \frac{k_+}{k_+(0)} = m \ln \left(\frac{1 + \mu C/K_R}{1 + C/K_R}\right) \quad (17)$$

and

$$\ln \frac{k_-}{k_-(0)} = m \ln \left(\frac{1 + \mu C/K_R}{1 + C/K_T}\right).$$

The corresponding formulas for the Scharf model, derived using transition-state theory (Eyring and Urry, 1965), are

$$\ln \frac{k_+}{k_+(0)} = m \frac{p-r}{kT} \frac{C}{C+K}$$

and

$$\ln \frac{k_-}{k_-(0)} = m \frac{p-r}{kT} \frac{C}{C+K}, \quad (18)$$

where p , equivalent to $kT \ln(\mu)$, is the negative of the change in the free energy of activation for switching upon binding one molecule of CheY**.

FITS TO THE MODELS

At each temperature, K_R and K_T were estimated from a nonlinear least-squares fit to Eq. 9. An example of such a fit is shown in Fig. 3. Similarly, values for K and r were estimated for each temperature, using the method of Scharf et al. (1998). The values for K_R , K_T , and K are shown in Fig. 4 A. Fig. 4 B shows r , the shift in standard free energy difference between the CW and CCW states per molecule of CheY** bound. A linear regression over the temperature range of 5–29°C gives the entropy and enthalpy contribution to this free energy shift of $-0.03kT/^\circ\text{C}$ and $0.10kT$, respectively, where k is Boltzmann's constant and T is 289 Kelvin ($= 16^\circ\text{C}$).

Fig. 5 shows a nonlinear least-squares fit to Eq. 17, which gives an estimate for the parameter μ . The transition parameter of the Scharf model, p , was estimated as in Scharf et al. (1998). Values of $kT \ln(\mu)$ and p are plotted as a function of temperature in Fig. 6. The model fits in the left and center columns of Fig. 1 were computed using the formulas

$$\text{CW bias} = \frac{k_+}{k_+ + k_-}$$

and

$$\text{Reversal frequency} = \frac{2k_+k_-}{k_+ + k_-},$$

where k_+ and k_- were determined from Eq. 17 (for the MWC model) or Eq. 18 (for the Scharf model).

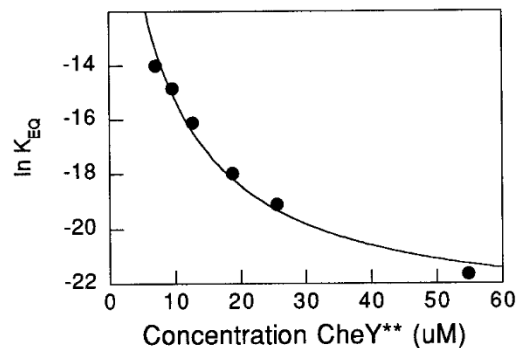


FIGURE 3 An example of a fit to Eq. 9, using data obtained at 29°C. The line corresponds to $K_R = 8.3 \mu\text{M}$ and $K_T = 3.4 \mu\text{M}$.

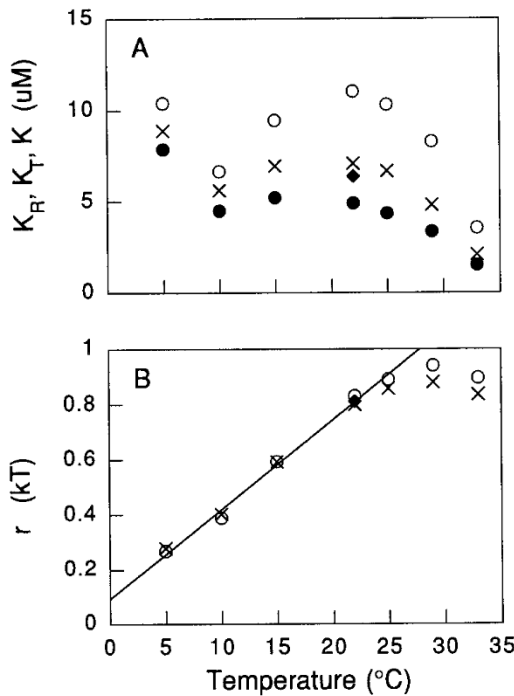


FIGURE 4 Values of dissociation constants (A) and energy shifts per molecule of CheY** bound (B) for the two models. (A) For the MWC model, \circ is K_R and \bullet is K_T . For the Scharf model \times is K , and \blacklozenge the value reported by Scharf et al. (1998). (B) For the MWC model, \circ is $kT \ln(K_R/K_T)$. For the Scharf model, \times is r , and \blacklozenge is the value reported by Scharf et al. (1998).

CONCLUSIONS

Both models assume that CheY** affects switching by binding to the motor, stabilizing the CW state and destabilizing the CCW state. In the MWC model, a shift in the difference in free energy between CW and CCW states arises because binding is tighter (the dissociation constant is smaller) in the CW state than in the CCW state, giving $r = kT \ln(K_R/K_T)$. In the Scharf model, r is a free parameter, and the reason for the shift is not specified. The dissociation constant is then an average of K_R and K_T , weighted by the

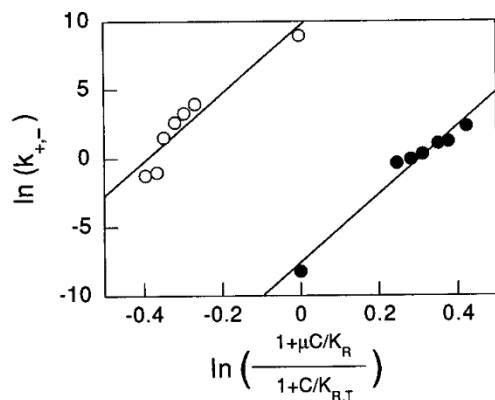


FIGURE 5 An example of a fit to Eq. 17, using data obtained at 29°C, with K_R and K_T equal to values determined in Fig. 3. $\mu = 1.61$.

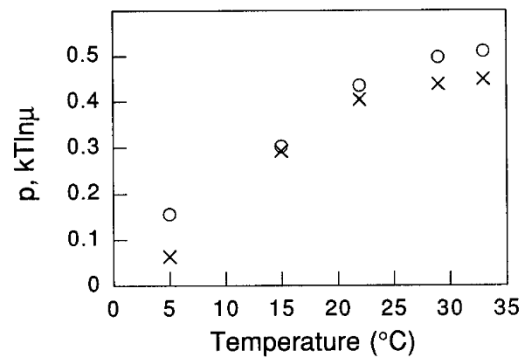


FIGURE 6 The shift in the activation energy for switching per molecule of CheY** bound shown as a function of temperature: for the MWC model, \circ is $kT \ln(\mu)$, and for the Scharf model, \times is p .

state occupancies. The MWC model treats allosteric molecules and their effectors as a closed system, whereas the Scharf model treats the flagellar motor as an open one. Scharf et al. do not claim to understand why CheY** has the effect that it does, so they proceed phenomenologically. Because r is of order kT (K_R is not very different from K_T), the two models give similar results; see Figs. 1, 4 B, and 6.

The energy shift per molecule of CheY** bound increases linearly from $\sim 0.3kT$ at 5°C to $\sim 0.9kT$ at 25°C. The entropy and enthalpy contributions to this shift are about $-0.031kT/^\circ\text{C}$ and $0.10kT$, respectively. It follows that at temperatures above 3°C, the entropic contribution to the free energy change dominates the enthalpic contribution. However, at temperatures above 25°C the energy shift per molecule of CheY** bound remains constant. The ineffectiveness of CheY** at higher temperatures is evident in Fig. 1. The cause remains unknown. During the experiments, it was noted that raising the temperature of the cells above 36°C caused an irreversible change in their behavior—upon returning to 22°C the bias retained the high-temperature value rather than reverting to its initial value. We speculate that the drop-off appearing in Fig. 4 B at high temperatures is related to the onset of this phenomenon.

We thank Rick Dahlquist for calling our attention to the MWC model and outlining its application to the flagellar motor, Karen Fahrner and Birgit Scharf for providing the CheY** strain, and Jeff Hoch and Will Ryu for helpful discussions.

This work was supported by the Rowland Institute for Science.

REFERENCES

- Abouhamad, W. N., D. Bray, M. Schuster, K. C. Boesch, R. E. Silversmith, and R. B. Bourret. 1998. Computer-aided resolution of an experimental paradox in bacterial chemotaxis. *J. Bacteriol.* 180:3757–3764.
- Alon, U., L. Camarena, M. G. Surette, B. Aguera y Arcas, Y. Liu, S. Leibler, and J. B. Stock. 1998. Response regulator output in bacterial chemotaxis. *EMBO J.* 17:4238–4248.
- Berg, H. C., and S. M. Block. 1984. A miniature flow cell designed for rapid exchange of media under highpower microscopy objectives. *J. Gen. Microbiol.* 130:2915–2920.

- Berg, H. C., and L. Turner. 1993. Torque generated by the flagellar motor of *Escherichia coli*. *Biophys. J.* 65:2201–2216.
- Blair, D. F. 1995. How bacteria sense and swim. *Annu. Rev. Microbiol.* 49:489–522.
- Block, S. M., J. E. Segall, and H. C. Berg. 1983. Adaptation kinetics in bacterial chemotaxis. *J. Bacteriol.* 154:312–323.
- Eisenbach, M., and S. R. Caplan. 1998. Bacterial chemotaxis: unsolved mystery of the flagellar switch. *Curr. Biol.* 8:R444–R446.
- Eyring, H., and D. W. Urry. 1965. Thermodynamics and chemical kinetics. In *Theoretical and Mathematical Biology*. T. H. Waterman and H. J. Morowitz, editors. Blarsdel Publishing Company, New York. 57–95.
- Falke, J. J., R. B. Bass, S. L. Butler, S. A. Chervitz, and M. A. Danielson. 1997. The two-component signaling pathway of bacterial chemotaxis: a molecular view of signal transduction by receptors, kinases, and adaptation enzymes. *Annu. Rev. Cell Dev. Biol.* 13:457–512.
- Hess, J. F., K. Oosawa, N. Kaplan, and M. I. Simon. 1988. Phosphorylation of three proteins in the signaling pathway of bacterial chemotaxis. *Cell.* 53:79–87.
- Hess, J. F., K. Oosawa, P. Matsumura, and M. I. Simon. 1987. Protein phosphorylation is involved in bacterial chemotaxis. *Proc. Natl. Acad. Sci. USA.* 84:7609–7613.
- Jones, C. J., R. M. Macnab, H. Okino, and S.-I. Aizawa. 1990. Stoichiometric analysis of the flagellar hook-(basal-body) complex of *Salmonella typhimurium*. *J. Mol. Biol.* 212:377–387.
- Khan, S., and H. C. Berg. 1983. Isotope and thermal effects in chemiosmotic coupling to the membrane ATPase of *Streptococcus*. *J. Biol. Chem.* 258:6709–6712.
- Liu, J., and J. S. Parkinson. 1989. Role of CheW protein in coupling membrane receptors to the intracellular signaling system of bacterial chemotaxis. *Proc. Natl. Acad. Sci. USA.* 86:8703–8707.
- Macnab, R. M. 1995. Flagellar switch. In *Two-Component Signal Transduction*. J. A. Hoch and T. J. Silhavy, editors. American Society for Microbiology, Washington, DC. 181–199.
- Macnab, R. M. 1996. Flagella and motility. In *Escherichia coli and Salmonella: Cellular and Molecular Biology*. F. C. Neidhardt, R. Curtiss, J. L. Ingraham, E. C. C. Lin, K. B. Low, B. Magasanik, W. S. Reznikoff, M. Riley, M. Schaechter, and H. E. Umbarger, editors. American Society for Microbiology, Washington, DC. 123–145.
- Monod, J., J. Wyman, and J.-P. Changeux. 1965. On the nature of allosteric transitions: a plausible model. *J. Mol. Biol.* 12:88–118.
- Oosawa, K., J. F. Hess, and M. I. Simon. 1988. Mutants defective in bacterial chemotaxis show modified protein phosphorylation. *Cell.* 53:89–96.
- Osborne, J. C., Jr., G. Palumbo, H. Bryan Brewer, Jr., and H. Edelhoch. 1976. The thermodynamics of the self-association of the reduced and carboxymethylated form of apoA-II from the human high density lipoprotein complex. *Biochemistry.* 15:317–320.
- Prasad, K., S. R. Caplan, and M. Eisenbach. 1998. Fumarate modulates bacterial flagellar rotation by lowering the free energy difference between the clockwise and counterclockwise states of the motor. *J. Mol. Biol.* 280:821–828.
- Ravid, S., and M. Eisenbach. 1984. Direction of flagellar rotation in bacterial cell envelopes. *J. Bacteriol.* 158:222–230.
- Scharf, B. E., K. A. Fahrner, L. Turner, and H. C. Berg. 1998. Control of direction of flagellar rotation in bacterial chemotaxis. *Proc. Natl. Acad. Sci. USA.* 95:201–206.
- Silversmith, R. E., and R. B. Bourret. 1999. Throwing the switch in bacterial chemotaxis. *Trends Microbiol.* 7:16–22.
- Sosinsky, G. E., N. R. Francis, D. J. DeRosier, J. S. Wall, M. N. Simon, and J. Hainfeld. 1992. Mass determination and estimation of subunit stoichiometry of the bacterial hook-basal body flagellar complex of *Salmonella typhimurium* by scanning transmission electron microscopy. *Proc. Natl. Acad. Sci. USA.* 89:4801–4805.
- Stock, J. B., and M. G. Surette. 1996. Chemotaxis. In *Escherichia coli and Salmonella: Cellular and Molecular Biology*. F. C. Neidhardt, R. Curtiss, J. L. Ingraham, E. C. C. Lin, K. B. Low, B. Magasanik, W. S. Reznikoff, M. Riley, M. Schaechter, and H. E. Umbarger, editors. American Society for Microbiology, Washington, DC. 1103–1129.
- Tanford, C. 1961. *Physical Chemistry of Macromolecules*. Wiley, New York. 532–535.
- Turner, L., S. R. Caplan, and H. C. Berg. 1996. Temperature-induced switching of the bacterial flagellar motor. *Biophys. J.* 71:2227–2233.
- Waelbroeck, M., E. Van Obberghen, and P. De Meyts. 1979. Thermodynamics of the interaction of insulin with its receptor. *J. Biol. Chem.* 254:7736–7740.
- Welch, M., K. Oosawa, S.-I. Aizawa, and M. Eisenbach. 1993. Phosphorylation-dependent binding of a signal molecule to the flagellar switch of bacteria. *Proc. Natl. Acad. Sci. USA.* 90:8787–8791.
- Welch, M., K. Oosawa, S.-I. Aizawa, and M. Eisenbach. 1994. Effects of phosphorylation, Mg^{2+} , and conformation of the chemotaxis protein CheY on its binding to the flagellar switch protein FliM. *Biochemistry.* 33:10470–10476.
- Wolfe, A. J., M. P. Conley, T. J. Kramer, and H. C. Berg. 1987. Reconstitution of signaling in bacterial chemotaxis. *J. Bacteriol.* 169:1878–1885.
- Wylie, D., A. Stock, C.-Y. Wong, and J. Stock. 1988. Sensory transduction in bacterial chemotaxis involves phosphotransfer between Che proteins. *Biochem. Biophys. Res. Commun.* 151:891–896.